

## Structural basis for action by diverse antidepressants on biogenic amine transporters

Hui Wang<sup>1</sup>, April Goehring<sup>1</sup>, Kevin H Wang<sup>1</sup>, Aravind Penmatsa<sup>1</sup>, Ryan Ressler<sup>1</sup>, Eric Gouaux<sup>1,2\*</sup>

### Supplementary Information

**Supplementary Figure 1.** Sequence alignment of wild-type LeuT and human serotonin transporter (hSERT), showing the regions of TM1, TM3, TM6, TM8 and TM10 that contribute to the primary or S1 binding site.

**Supplementary Figure 2.** Saturation binding of <sup>3</sup>[H]-labeled antidepressants to wild-type LeuT, LeuBAT Δ6 and Δ13 mutants measured by scintillation proximity assay.

**Supplementary Figure 3.** The Δ6 and Δ13 LeuBAT variants are not active in <sup>3</sup>H-dopamine or <sup>3</sup>H-serotonin transport.

**Supplementary Figure 4.** Fo-Fc omit electron density map of SSRIs, SNRIs, TCA and mazindol from 11 LeuBAT-drug complexes structures in the context of Δ13 and/or Δ6 mutants.

**Supplementary Figure 5.** Comparison of sertraline, duloxetine, desvenlafaxine and mazindol binding between the Δ5, Δ6 and Δ13 variants.

**Supplementary Figure 6.** Sodium and chloride ion binding sites in Δ13 LeuBAT.

**Supplementary Figure 7.** The binding of desvenlafaxine to the extracellular vestibule of LeuBAT is not affected by β-OG detergent.

**Supplementary Figure 8.** Comparison of pharmacology selectivity of LeuBAT with human dopamine transporter (hDAT), human serotonin transporter (hSERT) and human noradrenaline transporter (hNET).

**Supplementary Figure 9.** LeuBAT is a valid model for inhibitor binding to eukaryotic neurotransmitter sodium symporters by comparison of LeuBAT to the *Drosophila* dopamine transporter (dDAT).

**Supplementary Figure 10.** Mutations in the primary binding pockets of LeuBAT profoundly disrupt the binding of mazindol and sertraline yet preserve native, folded protein structure.

**Supplementary Table I.** Summary of LeuBAT mutant binding affinities to paroxetine and mazindol.

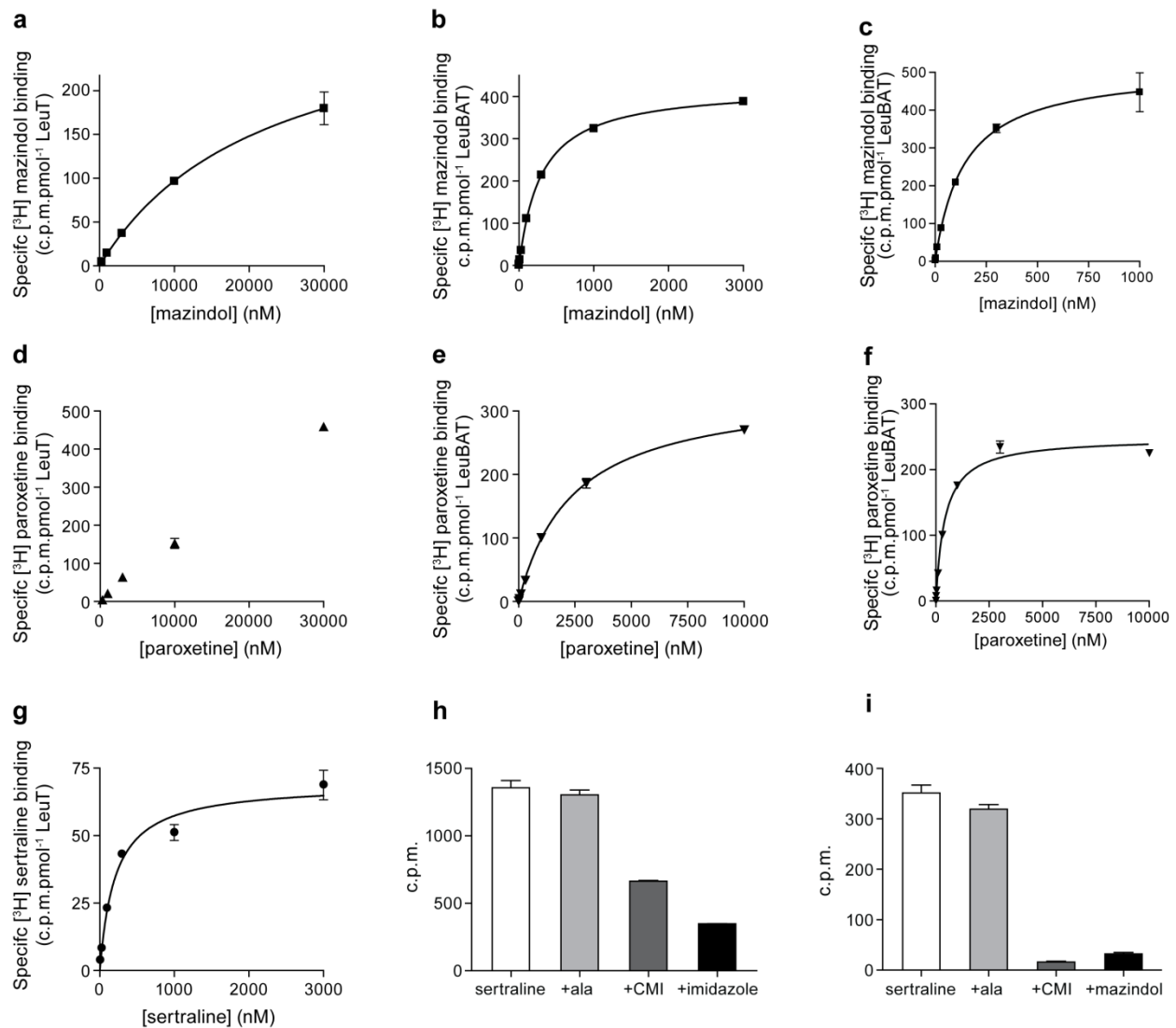
**Supplementary Table II.** Antidepressant inhibition constants for the  $\Delta 13$  LeuBAT mutant.

**Supplementary Table III.** Data collection and refinement statistics.

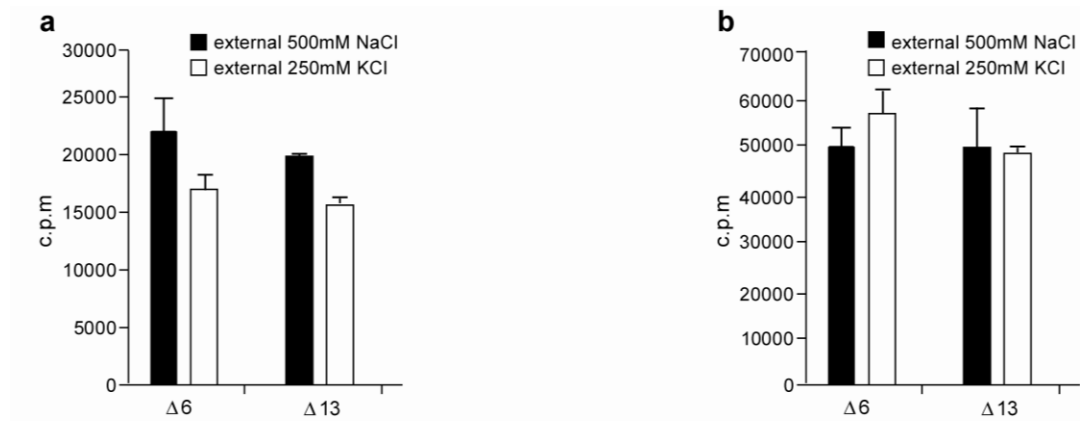
**Supplementary Table IV.** Summary of LeuBAT mutant binding affinities to sertraline.

TM1	LeuT	20	<sup>*</sup> GN <sup>*</sup> AVGL
	hSERT	94	GYAVDL
TM3	LeuT	104	V <sup>*</sup> AIYYV
	hSERT	172	IASYYN
TM6	LeuT	253	<sup>*</sup> FTL <sup>*</sup> SLGFGAIITYA <sup>**</sup>
	hSERT	335	FSLGPGFVLLAFA
TM8	LeuT	355	SSI <sup>*</sup> AIMQPM <sup>*</sup>
	hSERT	438	STFAGLEGV
TM10	LeuT	404	DFW <sup>**</sup> AGTI
	hSERT	493	EEYATGP

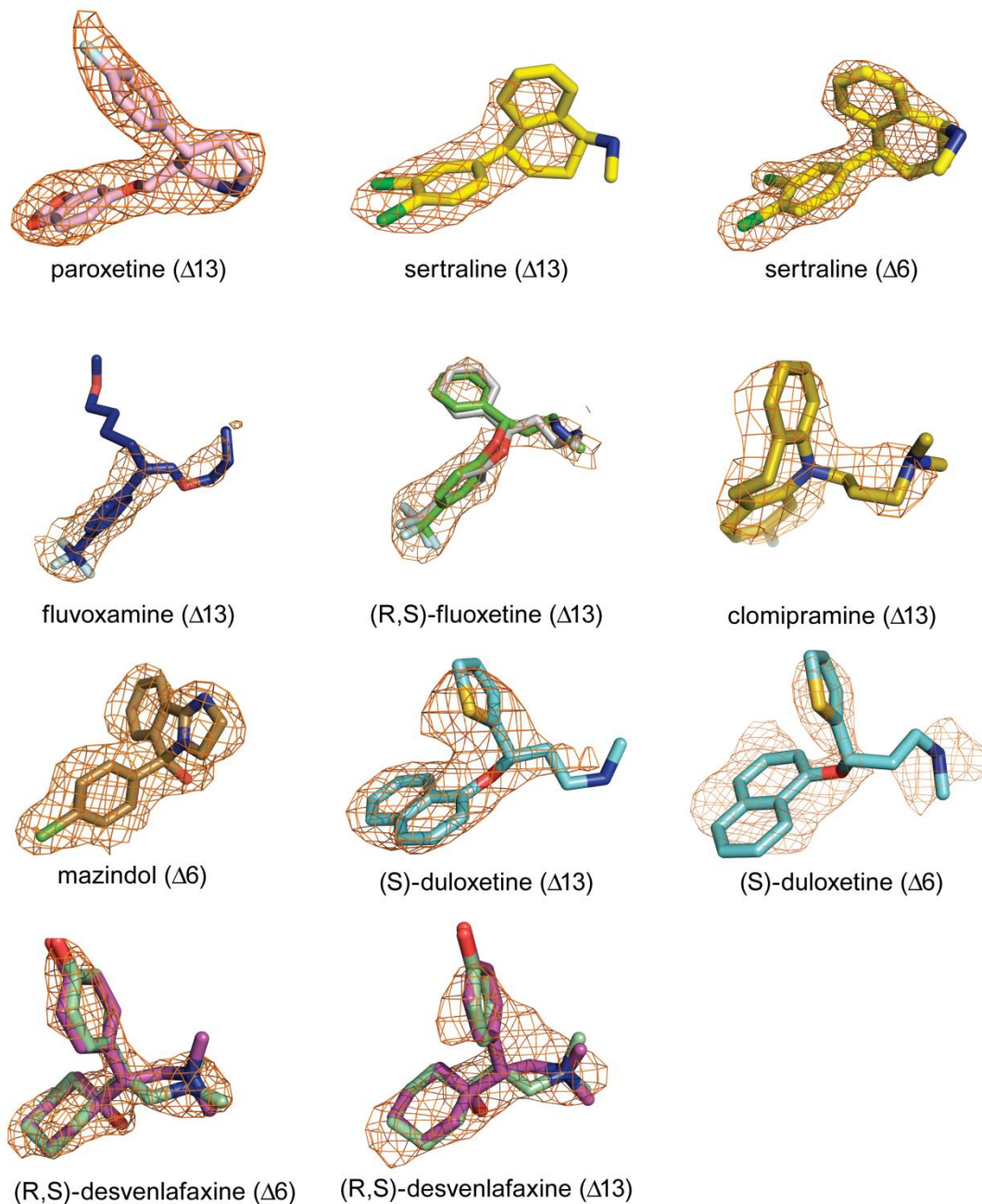
**Supplementary Figure 1.** Sequence alignment of wild-type LeuT and human serotonin transporter (hSERT), showing the regions of TM1, TM3, TM6, TM8 and TM10 that contribute to the primary or S1 binding site. Asterisks depict positions in which the residues of LeuT were mutated to the corresponding residues in hSERT.



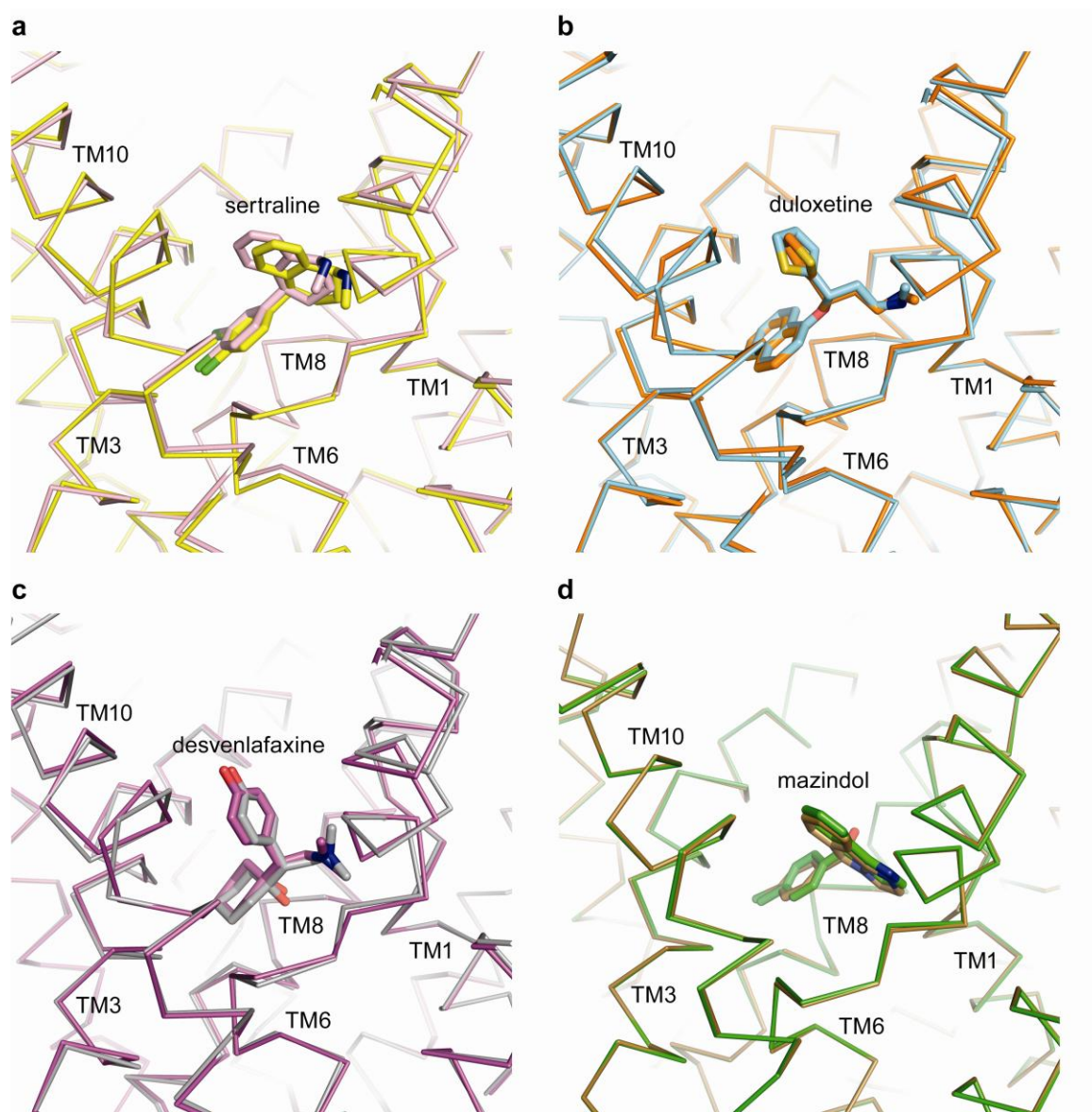
**Supplementary Figure 2.** Saturation binding of  $^3\text{H}$ -labeled antidepressants to wild-type LeuT, LeuBAT  $\Delta 6$  and  $\Delta 13$  mutants measured by scintillation proximity assay. **(a-c)** Saturation binding of  $^3\text{H}$ -mazindol to wild-type LeuT **(a)**,  $\Delta 6$  **(b)** and  $\Delta 13$  mutant **(c)**. The nonspecific binding was measured in the presence of 400 mM imidazole. **(d-f)** Saturation binding of  $^3\text{H}$ -paroxetine to wild-type LeuT **(d)**,  $\Delta 6$  **(e)** and  $\Delta 13$  mutant **(f)**. The nonspecific binding was measured in the presence of 400 mM imidazole (for **d**) and 0.1 mM mazindol (for **e** and **f**) **(g)** Saturation binding of  $^3\text{H}$ -sertraline to wild-type LeuT. The nonspecific binding was measured in the presence of 0.5 mM clomipramine (CMI). **(h)** Comparison of 3  $\mu\text{M}$   $^3\text{H}$ -sertraline binding to wild-type LeuT alone or with 5 mM Ala, 0.5 mM CMI and 400 mM imidazole. **(i)** Comparison of 30 nM  $^3\text{H}$ -sertraline binding to LeuBAT  $\Delta 13$  mutant alone or with 5 mM Ala, 0.5 mM CMI and 0.2 mM mazindol.



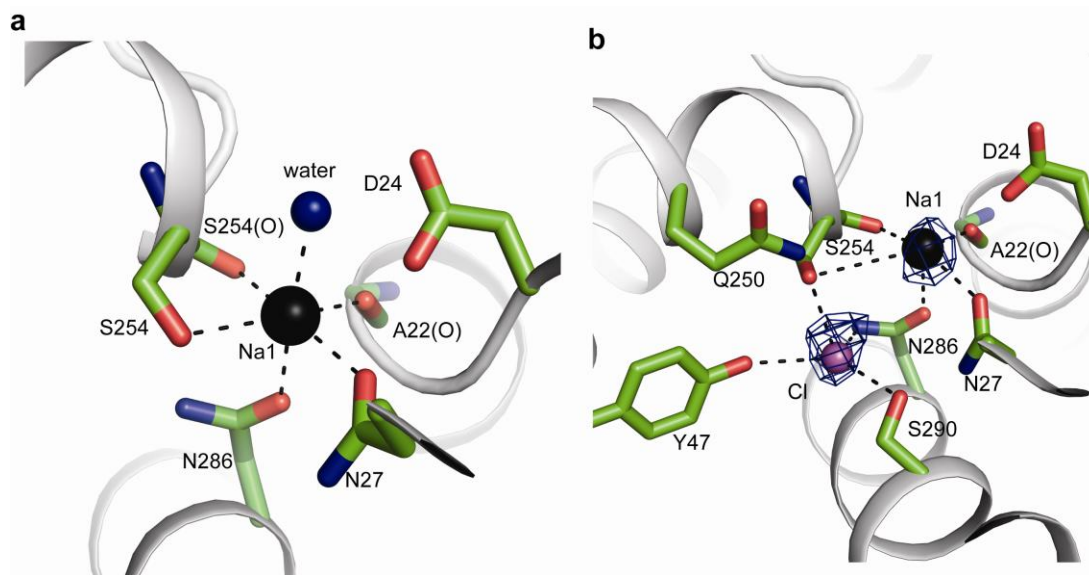
**Supplementary Figure 3.** The  $\Delta 6$  and  $\Delta 13$  LeuBAT variants are not active in  $^3\text{H}$ -dopamine or  $^3\text{H}$ -serotonin transport. **(a)** An attempt to measure  $^3\text{H}$ -dopamine transport by the  $\Delta 6$  and  $\Delta 13$  variants in the presence of a sodium gradient (filled bars). Background was estimated by way of a parallel measurement in which there is potassium (open bars) inside and outside the vesicles. **(b)** An attempt to measure  $^3\text{H}$ -serotonin uptake under similar conditions as described in (a). For both substrates, His-tagged  $\Delta 6$  and  $\Delta 13$  was reconstituted into lipid vesicles and the proteoliposomes were loaded with 20mM HEPES-Tris, pH 7.0 and 250mM KCl. Uptake was performed at 27 °C in either 20mM HEPES-Tris, pH7.0, 500mM NaCl, 1 $\mu$ M valinomycin, 1mM  $^3\text{H}$ -neurotransmitter or in 20mM HEPES-Tris pH7.0, 250mM KCl, 1 $\mu$ M valinomycin, 1mM  $^3\text{H}$ -neurotransmitter. Time points were taken at 10 min. The results are an average of three measurements and the error bars represent s.e.m.



**Supplementary Figure 4.** Fo-Fc omit electron density maps of SSRIs, SNRIs, TCA and mazindol from 11 LeuBAT-drug complexes structures in the context of the  $\Delta 13$  and/or  $\Delta 6$  mutants. The maps were contoured at  $2.5\sigma$ . For fluoxetine and desvenlafaxine, both (R)- and (S)-enantiomer were fit into the densities.

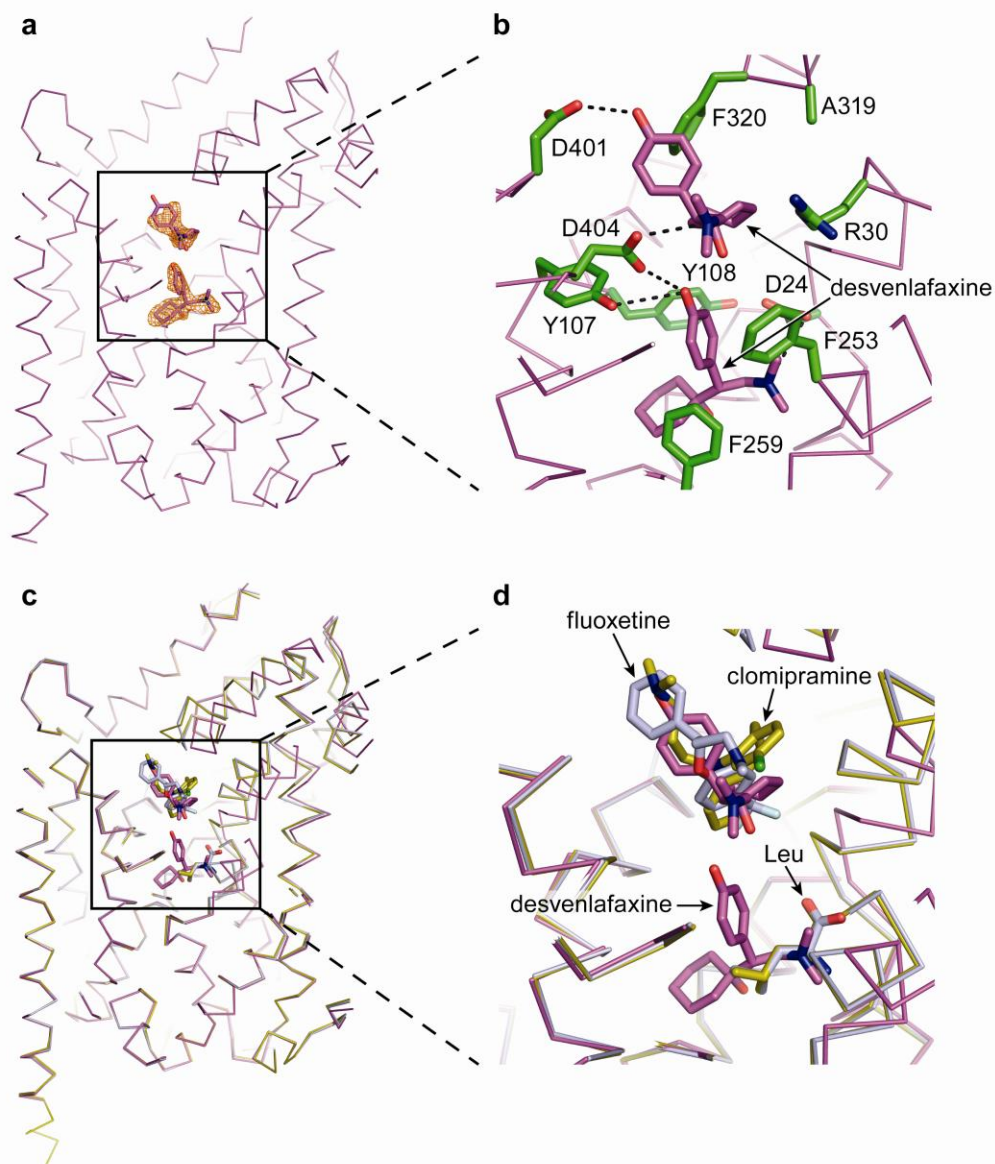


**Supplementary Figure 5.** Comparison of sertraline, duloxetine, desvenlafaxine and mazindol binding between the  $\Delta 5$ ,  $\Delta 6$  and  $\Delta 13$  variants. The superimpositions were performed to fit all atoms between these structures. **(a)** Structural comparison of sertraline binding between  $\Delta 13$  (yellow) and  $\Delta 6$  mutants (pink). **(b)** Structural comparison of duloxetine binding between  $\Delta 13$  (cyan) and  $\Delta 6$  mutants (orange). **(c)** Structural comparison of desvenlafaxine binding between  $\Delta 13$  (purple) and  $\Delta 6$  mutants (gray). **(d)** Structural comparison of mazindol binding between  $\Delta 6$  (sand) and  $\Delta 5$

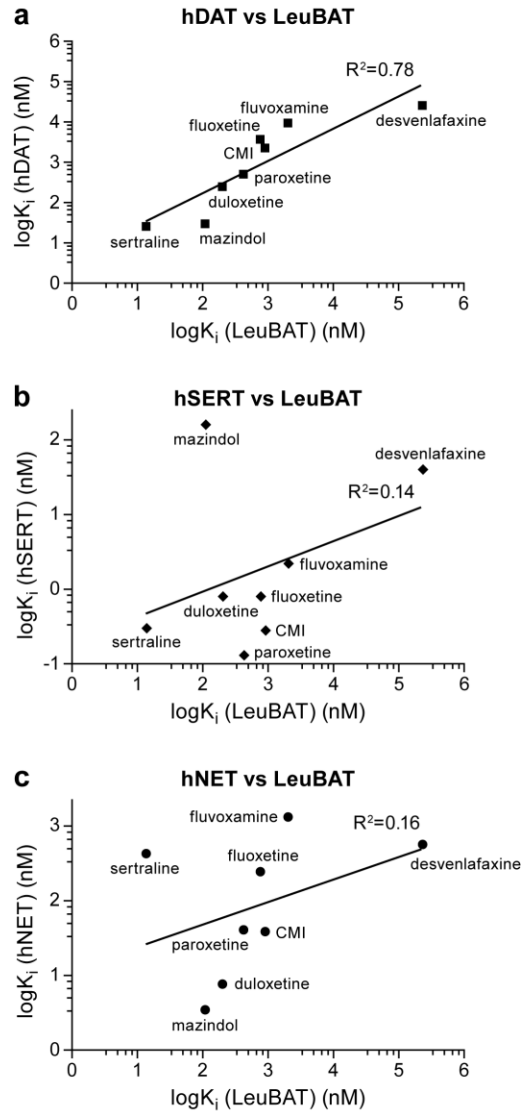


**Supplementary Figure 6.** Sodium and chloride ion binding sites in  $\Delta 13$  LeuBAT. **(a)** The coordination environment of Na1 in  $\Delta 13$  LeuBAT-desvenlafaxine. **(b)** The coordination environment of chloride in  $\Delta 13$  LeuBAT-paroxetine (chain B). The blue mesh depicts the Fo-Fc omit electron density maps of Cl<sup>-</sup> and Na<sup>+</sup> contoured at  $3\sigma$ . Key residues are shown as green sticks. Na<sup>+</sup>, Cl<sup>-</sup> and a solvent molecule modeled as water are shown as black, purple and blue spheres, respectively.

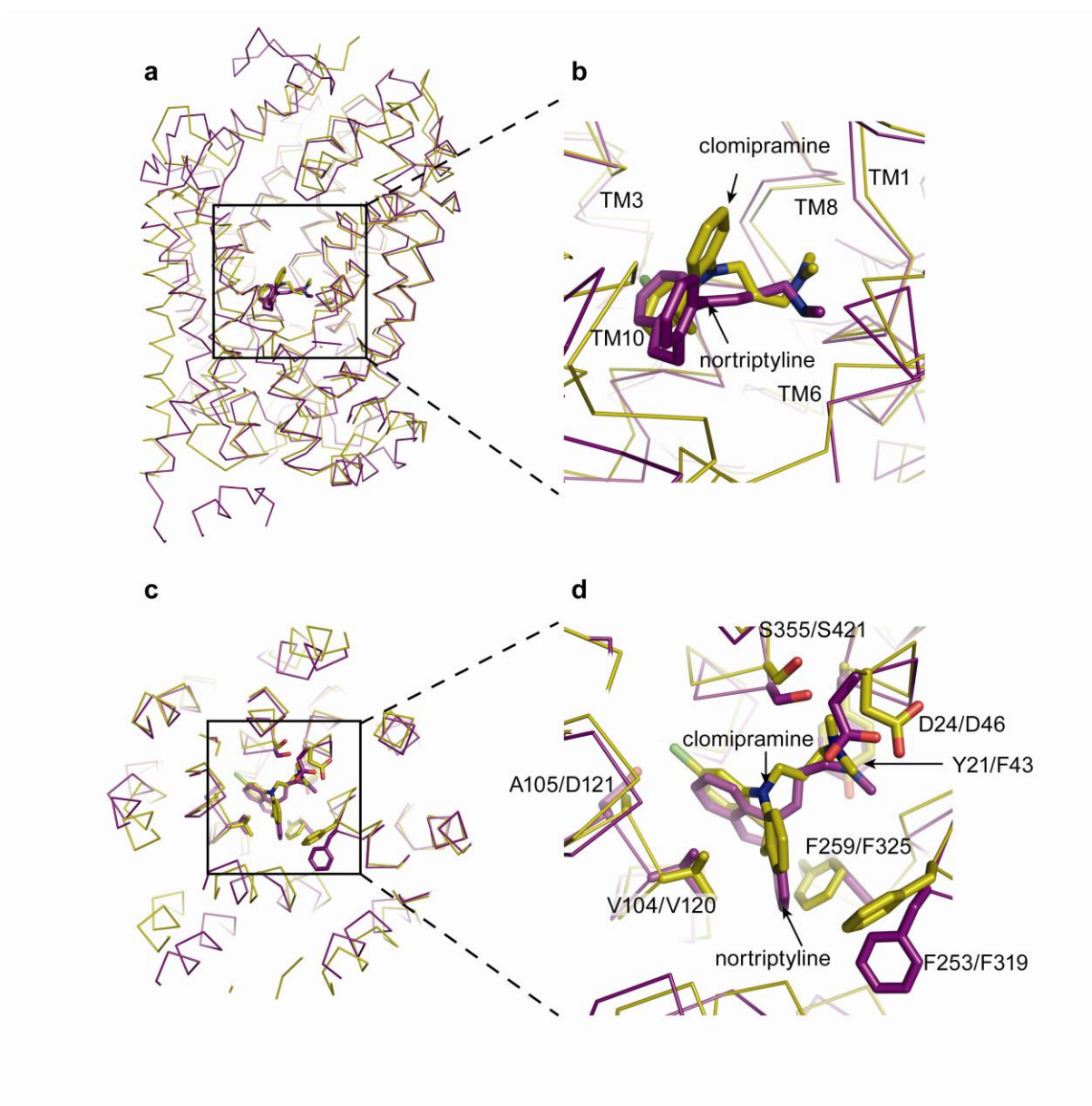




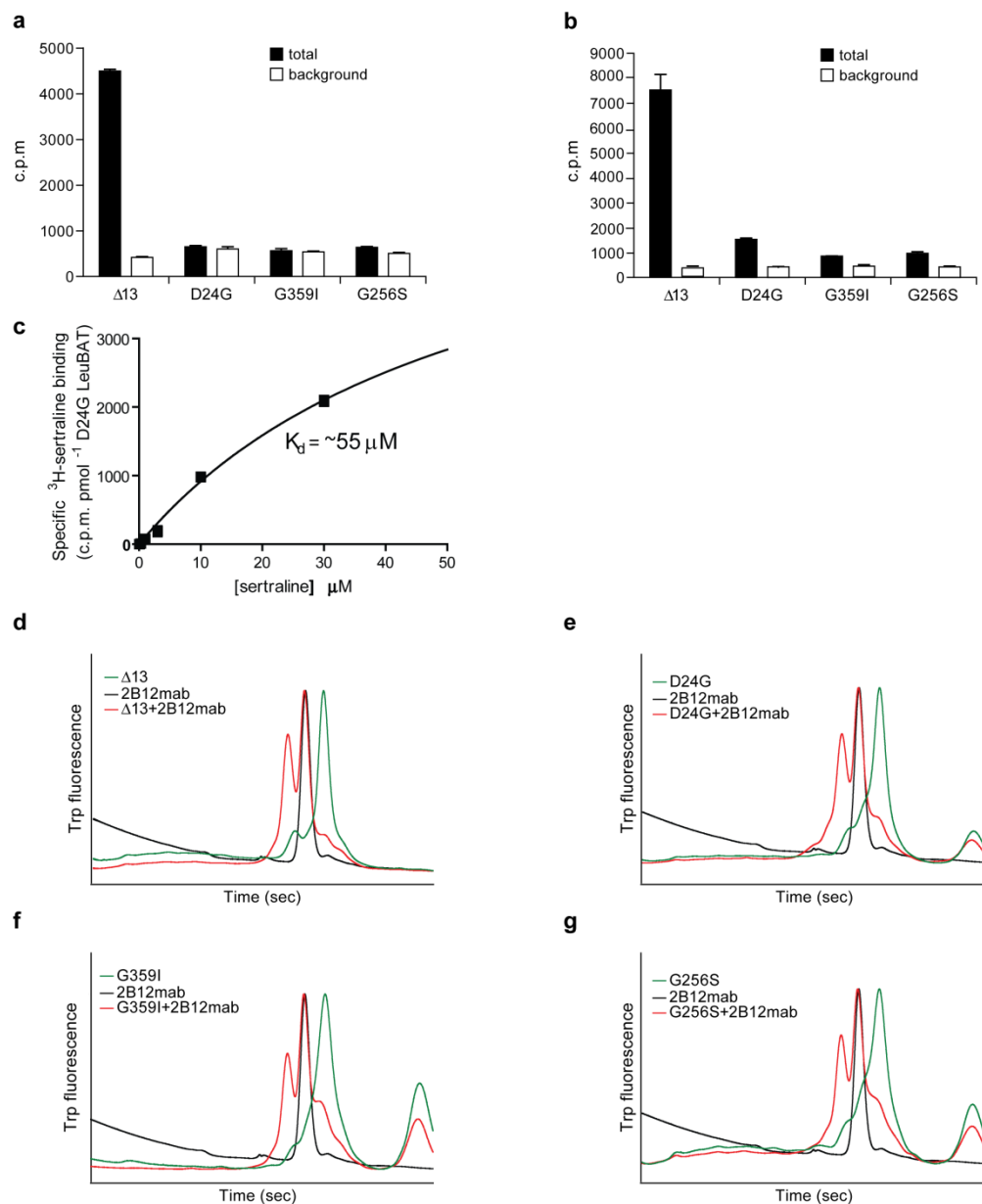
**Supplementary Figure 7.** The binding of desvenlafaxine to the extracellular vestibule of LeuBAT is not affected by  $\beta$ -OG detergent. **(a)** Two desvenlafaxine molecules (purple) were identified in the structure of the  $\Delta 6$  mutant (purple) in complex with desvenlafaxine. The orange meshes depict the Fo-Fc omit electron densities of desvenlafaxine contoured at  $3\sigma$ . **(b)** Close up of the desvenlafaxine binding sites in the primary binding pocket and extracellular vestibule. Key residues are shown as green sticks. **(c)** The superimposition of  $\Delta 6$ -desvenlafaxine, wild-type LeuT-flouxetine (PDB 3GWV) (light blue) and wild-type LeuT-CMI (PDB 2Q6H) (olive) complexes. The bound leucine, flouxetine and CMI are shown as sticks. **(d)** Close up of the drug binding sites in the extracellular vestibule as well as in the primary binding pocket.



**Supplementary Figure 8.** Comparison of pharmacology selectivity of LeuBAT with human dopamine transporter (hDAT), human serotonin transporter (hSERT) and human noradrenaline transporter (hNET). **(a)** Plot of drugs inhibition constants for hDAT against inhibition constants for  $\Delta 13$  LeuBAT. The  $R^2$  (goodness-of-fit of linear regression) value is 0.78. **(b)** Plot of drugs inhibition constants for hSERT against inhibition constants for  $\Delta 13$  LeuBAT. The  $R^2$  (goodness-of-fit of linear regression) value is 0.14, but the  $R^2$  would be 0.71 if the mazindol point is left out. **(c)** Plot of drugs inhibition constants for hNET against inhibition constants for  $\Delta 13$  LeuBAT. The  $R^2$  value is 0.16, but the  $R^2$  would be 0.50 if the sertraline point is left out.



**Supplementary Figure 9.** LeuBAT is a valid model for inhibitor binding to eukaryotic neurotransmitter sodium symporters by comparison of LeuBAT to the *Drosophila* dopamine transporter (dDAT). **(a)** The superimposition of LeuBAT-CMI (olive) with dDAT-nortriptyline (purple) viewed from membrane plane. The r.m.s deviation for C $\alpha$  atoms is 1.77 Å. CMI and nortriptyline are depicted as sticks. **(b)** Close up of the drug binding pocket in panel **(a)**. **(c)** The superimposition of LeuBAT-CMI (olive) with dDAT-nortriptyline (purple) viewed from extracellular side. Key residues are shown as sticks. **(d)** Close up of the drug binding pocket in panel **(c)**. The residue numbering follows LeuBAT and dDAT, respectively.



**Supplementary Figure 10.** Mutations in the primary binding pockets of LeuBAT profoundly disrupt the binding of mazindol and sertraline yet preserve native, folded protein structure. **(a)** Comparison of the binding of [<sup>3</sup>H]-mazindol to Δ13, Δ13D24G, Δ13G256S and Δ13G359I mutants (n=3). **(b)** Comparison of the binding of [<sup>3</sup>H]-sertraline to Δ13, Δ13D24G, Δ13G256S and Δ13G359I mutants (n=3). **(c)** Saturation binding of <sup>3</sup>H-sertraline to Δ13D24G mutant yields and approximate  $K_d$  of 55 μM. **(d-g)** The 2B12 monoclonal antibody (mab) that binds to the folded, native state of LeuT shifts the peaks of the Δ13 **(d)**, Δ13D24G **(e)**, Δ13G359I **(f)** and Δ13G256S **(g)** variants, thus demonstrating that these proteins are folded into a native conformation. In panels **d-g**, the prominent peaks of the green traces are LeuBAT, the peaks of the black traces are the mab, and in the red traces, the left peak is that of the LeuBAT-mab complex while the peak on the right is excess, uncomplexed mab.

**Supplementary Table I. Summary of LeuBAT mutant binding affinities to paroxetine and mazindol (n=3,  $\pm$ s.e.m)**

	wild-type	$\Delta$ 5	$\Delta$ 6	$\Delta$ 8	$\Delta$ 10	$\Delta$ 12A	$\Delta$ 12B	$\Delta$ 13
		S256G I359G G24D N21Y T254S	S256G I359G G24D N21Y T254S Y265F	S256G I359G G24D N21Y T254S Y265F A261V I262L	S256G I359G G24D N21Y T254S Y265F A261V I262L G408T T409G	S256G I359G G24D N21Y T254S Y265F A261V I262L G408T T409G E290S P362G	S256G I359G G24D N21Y T254S Y265F A261V I262L G408T T409G E290S I106S	S256G I359G G24D N21Y T254S Y265F A261V I262L G408T T409G E290S P362G I106S
<b>K<sub>d</sub> (nM) (paroxetine)</b>	<b>unmeasurable</b>	<b>2336<math>\pm</math>285</b>	<b>2407<math>\pm</math>106</b>	<b>1851<math>\pm</math>177</b>	<b>780<math>\pm</math>55</b>	<b>696<math>\pm</math>34</b>	<b>417<math>\pm</math>35</b>	<b>431<math>\pm</math>24</b>
<b>K<sub>d</sub> (nM) (mazindol)</b>	<b>22271<math>\pm</math>5398</b>	<b>295<math>\pm</math>7</b>	<b>318<math>\pm</math>10</b>	<b>N/A</b>	<b>N/A</b>	<b>N/A</b>	<b>N/A</b>	<b>112<math>\pm</math>18</b>

**Supplementary Table II. Antidepressant inhibition constants for  $\Delta 13$  LeuBAT mutant (n=3,  $\pm$ s.e.m)**

drugs	sertraline	fluoxetine	fluvoxamine	duloxetine	clomipramine	desvenlafaxine
<b>K<sub>i</sub> (nM)</b>	14 $\pm$ 2	778 $\pm$ 76	2070 $\pm$ 272	205 $\pm$ 15	920 $\pm$ 76	235500 $\pm$ 82352

**Supplementary Table III. Data collection and refinement statistics<sup>a</sup>**

	<b>Δ13-paroxetine</b>	<b>Δ13-sertraline</b>	<b>Δ6-sertraline</b>	<b>Δ13-fluvoxamine</b>
<b>Data collection</b>				
Wavelength (Å)	0.979	0.979	1.000	0.979
Space group	P2 <sub>1</sub>	C2	C2	C2
Cell dimensions a, b, c (Å) α, β, γ (°)	88.4, 92.1, 84.8 90.0, 94.8, 90.0	89.1, 87.9, 82.0 90.0, 95.5, 90.0	86.2, 87.3, 81.0 90.0, 94.5, 90.0	90.8, 88.1, 81.5 90.0, 94.8, 90.0
Resolution (Å)	40.0-2.9 (3.0-2.9)	40.0-3.2 (3.31-3.2)	40.0-2.25 (2.33-2.25)	51.3-2.9 (3.08-2.9)
R <sub>merge</sub>	0.11 (0.73)	0.12 (0.64)	0.11 (0.66)	0.11 (0.55)
I/σI	11 (1.2)	14.4 (2.1)	13.6 (1.4)	5.2 (1.4)
Completeness (%)	98.8 (95.0)	94.7 (80.3)	99.2 (94.0)	99.9 (100)
Redundancy	3.7 (3.4)	2.9 (2.3)	3.9 (3.0)	3.9 (4.0)
<b>Refinement</b>				
Resolution (Å)	37.3-2.9	31.5-3.2	39.2-2.24	45.2-2.9
No. reflections	30223	9862	28409	14298
R <sub>work</sub> / R <sub>free</sub>	0.219/0.241	0.213/0.264	0.199/0.234	0.230/0.272
No. atoms				
Protein	7909	3944	4011	3964
Ligand/ion	2 paroxetine/4Na/1Cl	1 sertraline/2Na	1 sertraline/2Na	1fluvoxamine/2Na
Water	3	2	77	1
B-factors (Å <sup>2</sup> )				
Protein	51.5	45.7	41.9	51.7
Ligand/ion	46.0	37.3	36.3	46.9
Water	37.2	32.5	43.7	39.0
R.m.s. deviations				
Bond lengths (Å)	0.011	0.009	0.009	0.009
Bond angles (°)	0.827	0.782	0.808	0.781

<sup>a</sup> Values in parentheses correspond to the highest resolution shells.

**Supplementary Table III. Data collection and refinement statistics (continued)**

	$\Delta$ 13-duloxetine	$\Delta$ 6-duloxetine	$\Delta$ 13-desvenlafaxine	$\Delta$ 6- desvenlafaxine
<b>Data collection</b>				
Wavelength (Å)	0.979	1.000	0.979	1.000
Space group	C2	P2 <sub>1</sub>	C2	C2
Cell dimensions a, b, c (Å) $\alpha$ , $\beta$ , $\gamma$ (°)	87.9, 88.4, 81.3 90.0, 94.8, 90.0	84.4 , 92.2, 88.3 90.0, 94.1, 90.0	87.6, 88.0, 81.4 90.0, 95.0, 90.0	87.7, 87.0, 81.4 90.0, 94.7, 90.0
Resolution (Å)	40.0-3.1 (3.2-3.1)	40.0-2.3(2.88-2.30)	40.0-2.85(2.95-2.85)	40.0-2.30 (2.38-2.30)
R <sub>merge</sub>	0.12 (0.52)	0.09 (0.78)	0.09 (0.49)	0.09 (0.59)
I/ $\sigma$ I	11.3 (1.4)	23.4 (1.8)	17.9 (1.9)	16.9 (1.6)
Completeness (%)	95.9 (80.4)	99.9 (99.8)	96.9 (82.9)	99.3 (94.9)
Redundancy	2.9 (2.4)	4.0 (4.1)	3.5 (3.1)	3.6 (3.1)
<b>Refinement</b>				
Resolution (Å)	38.8-3.1	40.0-2.30	38.7-2.85	39.9-2.29
No. reflections	10993	59970	14009	27064
R <sub>work</sub> / R <sub>free</sub>	0.214/0.235	0.213/0.244	0.210/0.252	0.201/0.228
No. atoms				
Protein	4005	8022	3962	4011
Ligand/ion	1 duloxetine/2Na	2 duloxetine/4Na	1desvenlafaxine/ 2Na	2desvenlafaxine/ 2Na
Water	1	119	2	73
<b>B-factors (Å<sup>2</sup>)</b>				
Protein	53.1	44.4	42.9	42.3
Ligand/ion	41.2	37.2	34.7	42.8
Water	49.87	46.8	34.8	46.8
<b>R.m.s. deviations</b>				
Bond lengths (Å)	0.010	0.004	0.009	0.007
Bond angles (°)	0.942	1.031	0.803	0.768



**Supplementary Table III. Data collection and refinement statistics (continued)**

	$\Delta$ 13-fluoxetine	$\Delta$ 13-CMI	$\Delta$ 6-mazindol	$\Delta$ 5-mazindol
<b>Data collection</b>				
Wavelength (Å)	0.979	0.979	1.000	1.000
Space group	C2	C2	P2 <sub>1</sub>	P2 <sub>1</sub>
Cell dimensions a, b, c (Å) $\alpha$ , $\beta$ , $\gamma$ (°)	85.6, 87.8, 80.8 90.0, 94.5, 90.0	88.5, 88.8, 81.2 90.0, 94.4, 90.0	84.3, 92.8, 87.5 90.0, 93.7, 90.0	84.2, 92.1, 87.8 90.0, 93.5, 90.0
Resolution (Å)	40.0-3.3 (3.4-3.3)	40.0-3.3 (3.42-3.3)	50.0-2.5 (2.59-2.5)	40.0-2.7 (2.8-2.7)
R <sub>merge</sub>	0.15 (0.52)	0.11 (0.95)	0.10 (0.53)	0.10 (0.69)
I/ $\sigma$ I	7.7 (1.3)	10.4 (1.1)	19.8 (1.7)	15.8 (1.4)
Completeness (%)	93.4 (80.1)	89.8 (74.9)	99.9 (99.4)	99.5 (95.8)
Redundancy	2.9 (2.6)	2.7 (2.8)	4.1 (3.9)	3.5 (3.2)
<b>Refinement</b>				
Resolution (Å)	38.5-3.3	38.9-3.29	41.0-2.50	38.9-2.69
No. reflections	8394	8538	46598	37062
R <sub>work</sub> / R <sub>free</sub>	0.214/0.250	0.246/0.261	0.204/0.233	0.199/0.236
No. atoms				
Protein	3955	4005	8044	8024
Ligand/ion	1 fluoxetine/2Na	1CMI/2Na	2 mazindol/4Na	2 mazindol/4Na
Water	2	3	52	54
B-factors (Å <sup>2</sup> )				
Protein	36.5	127.4	42.5	47.1
Ligand/ion	34.7	114.6	36.7	36.2
Water	22.6	98.5	43.9	45.1
R.m.s. deviations				
Bond lengths (Å)	0.009	0.010	0.009	0.008
Bond angles (°)	0.775	0.871	1.128	1.130

**Supplementary Table IV. Summary of LeuBAT mutant binding affinities to sertraline (n=3,  $\pm$ s.e.m)**

<b>Validation mutants</b>	$\Delta$ 13Y21A	$\Delta$ 13D24E	$\Delta$ 13F259Y	$\Delta$ 13S355T
<b>K<sub>d</sub> (nM) (sertraline)</b>	4630 $\pm$ 789	1525 $\pm$ 131	247 $\pm$ 11	20924 $\pm$ 5391